New concept for a photonic switch

Ervin Goldfain

R & D Department, Optical Systems Division
Cambridge Instruments Inc., Buffalo, NY 14240

ABSTRACT

The paper reveals a new operating principle for a planar photonic transistor in which no electronic components or nonlinear optical modules are used for digital switching.

The author investigates the design constraints associated with the switching function, the contribution of the "noise" factors as well as the integration of the switch in a logic processor.

1. INTRODUCTION

The optical computing field is emerging as a dynamic area of interest and its foundations lie mainly in the use of either nonlinear optical materials (NLO) or electrooptic/acoustooptic modulators.

As it is well known the optical bistability associated with NLO relates to the manipulation of the beam parameters as a result of an appropriate change in the refractive index of these media.

The external modulation of the beam implies a physical interaction between the wavefront and the excitation field which assists the switching function.

The present paper explores the design of a pure planar optical switch without any nonlinear component or modulator. Such a device has several major potential merits over the "traditional" optical flip-flop:

1) the computation speed is practically limited to the speed of light in the dielectric waveguide.

2) the switch is immune to electromagnetic/acoustic interference or crosstalk.

3) the switch is practically insensitive to environmental fluctuations in temperature or pressure.

4) the output signal does not display any saturation - regardless of the time of use - which makes the switching function fully repeatable.

The operating principle of our novel device is based on the shift of the Fraunhoffer diffraction pattern due to the superposition of two coherent wavefronts at the focal plane location. The technique is fully compatible with the requirements of parallel optical processing.

By definition, a device is said to be optically bistable if two stable outputs can be generated for the same value of the input over a certain input range [1]. The transmission characteristic of a bistable device is illustrated in Fig. 1.

For intensities close to I_G a minute change of the input induces a jump of the output (bifurcation). This switch does not perform as a memory gate since no hysteresis is present. In addition to the switching function, the device can be used either as an optical limiter (a further variation beyond I'_G does not affect the output) or as an optical discriminator (only below I_G the input is highly attenuated) [1].

Let us mention that optical computing techniques based on interference fringe shifting were investigated before in conjunction with NLO [2]. The main disadvantages associated with these designs relate to the access time of the photorefractive effect as well as to the need of external control blocks.

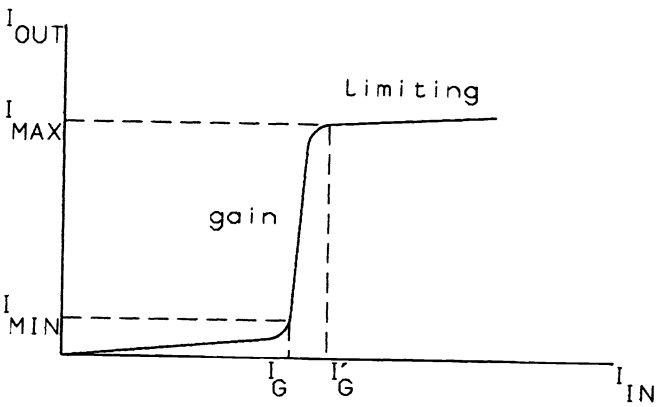

FIG.1

2. DESCRIPTION OF THE SWITCHING FUNCTION

The procedure described below is similar to the classical setup of double slit interference (Young's experiment).

Consider two monochromatic TEM_{oo} wavefronts emerging from two laser diodes and having the standard Gaussian intensity profile. The relays "R_1" and "R_2" project the beam waists onto a screen provided with two narrow rectangular slits as illustrated in Fig. 2. The far-field diffraction pattern is imaged at the back focal plane of a high resolution objective "0". A specially coated target with a high transmission ratio is placed on this plane and a third relay "R_3" projects the image of the target at infinity. The light intensity on the output beam axis is taken as the binary logic variable. When the second incident beam is missing, the diffraction pattern is given by the Fourier transform of the first wavefront through a single slit "S_1". In this case the peak value of the amplitude is detected at the paraxial image location of "S_1" through "0". As soon as the second beam is activated, the diffraction pattern displays a maximum fringe on the optical axis of "0" and a transverse modulation in amplitude [3] (Fig. 4).

It is apparent now that if the target is placed at a zero minima of the two-slit pattern, the relay "R_3" will pick up either a "0" or a "1" signal depending on how the incident beams are being used.

In the above setup "S_1" provides the "reference" beam and is permanently activated while "S_2" operates as the input signal.

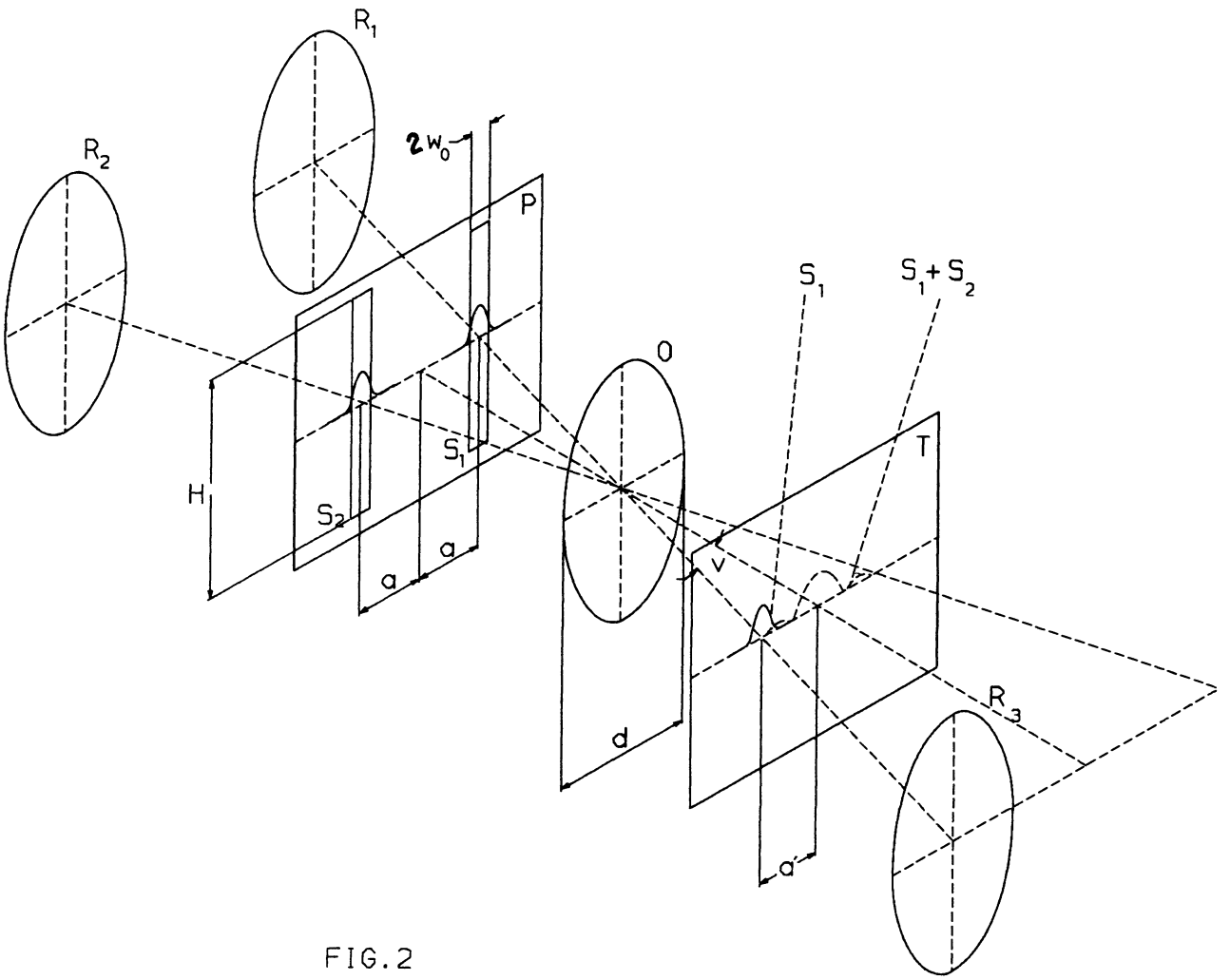

FIG.2

This configuration is suitable to be integrated in a planar envelope as shown (Fig. 4) in which:

a) all the optical components are geodesic microlenses.

b) the screen is replaced by two identical microslits etched onto the dielectric substrate (field stops). If the width of these stops is comparable with the size of the beam waist (truncation at $1/e^2$ of the peak value), there is no cutoff of the radiant energy over the beam cross section and the laser wavefront diverges as a result of natural diffraction [4] [5].

c) the high transmission target is a spherical protrusion representing a graded index microlens.

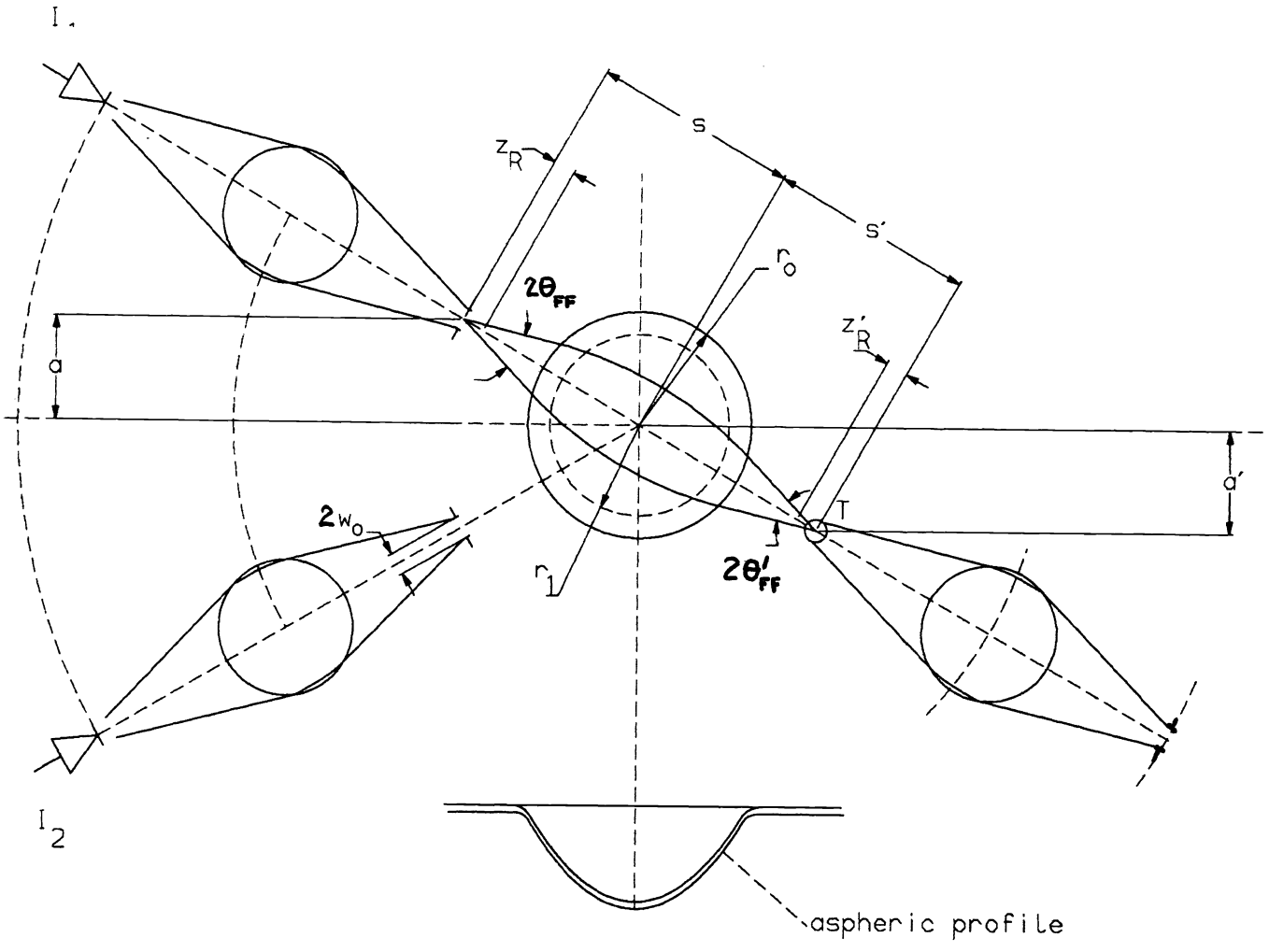

FIG.3

To set the frame of the analysis the following assumptions are made:

a) the incident beams are perfectly monochromatic which means infinite coherence time and zero linewidth:

$$\Delta\lambda \to 0 \tag{1}$$

b) the OPD's involved in the fringe pattern formation are much smaller than the coherence length:

$$\delta << \ell_{COH} \tag{2}$$

c) the peak intensities are equal for both beams:

$$I_1 = I_2 \tag{3}$$

d) all the optical components are diffraction limited and imaging is performed purely stigmatic according to the laws of Gaussian optics.

e) the width of the slits coincide with the beam waists at the screen location.

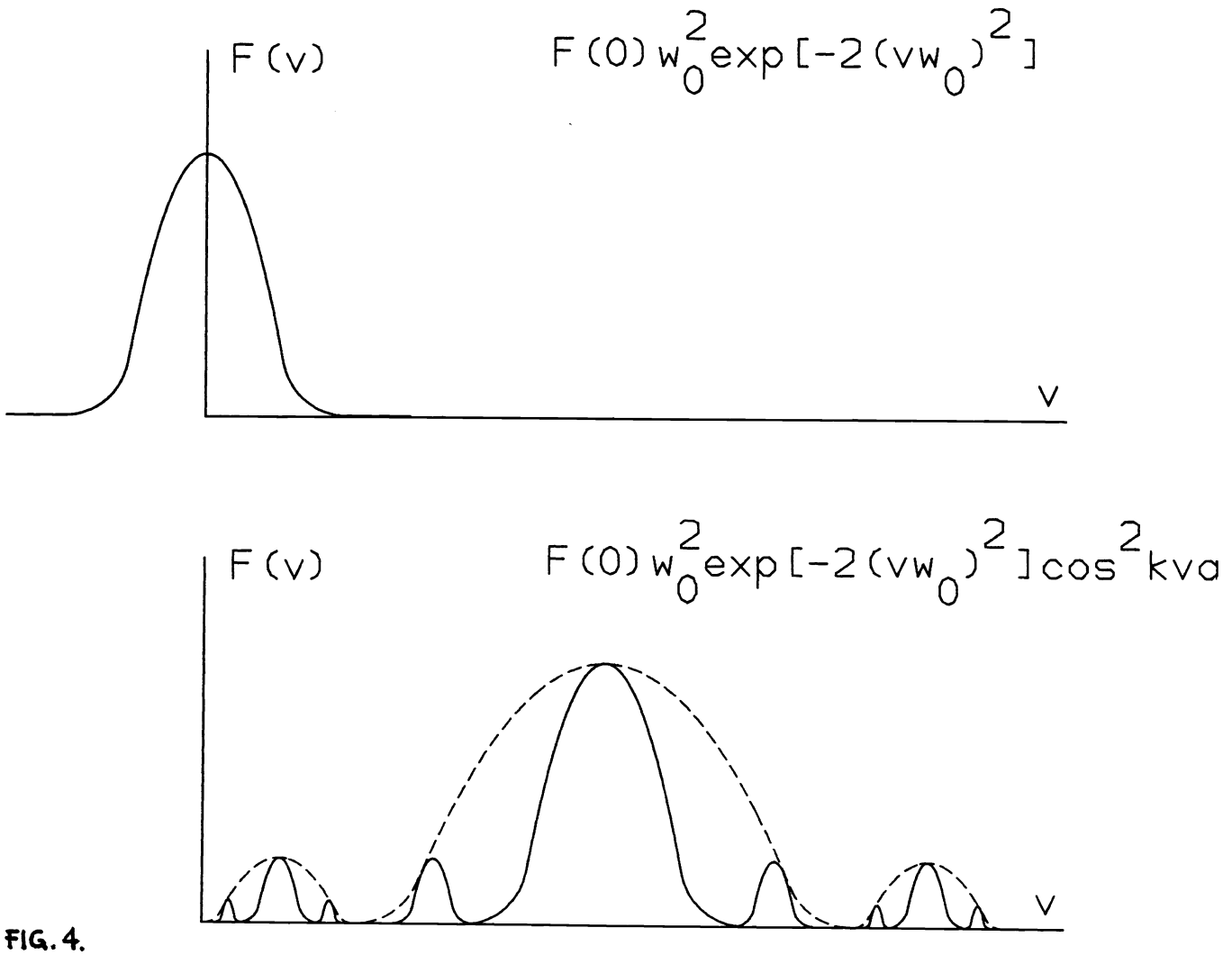

FIG. 4.

3. DESIGN OF THE PHOTONIC SWITCH

As it is known, one way to balance the spherical aberration of a geodesic lens for high apertures is to give an aspheric shape to the depression profile [7]. Because the geodesic lenses have radial symmetry they image concentric circles onto one another and are optically equivalent to generalized Luneburg lenses [11]. As it is also known, the TEM_{oo} output exhibits the minimum diffraction loss, the minimum beam spread and has the cylindrical Gaussian intensity distribution:

$$I(r) = I(o) \exp\left(-\frac{2r^2}{w^2}\right) = \frac{2P}{\pi w^2} \exp\left(-\frac{2r^2}{w^2}\right) \tag{4}$$

where the waist is a function of the propagation distance $w = w(s)$ and P stands for the total power of the beam.

When only the reference beam is operating, the diffraction pattern is is given by [13]:

$$F(v) = F(o) w_o^2 \exp\left[-2(vw_o)^2\right] \tag{5}$$

When both slits are operating, the resulting pattern depends on the phase shift of the wavefronts with respect to the optical axis of the objective "0". Therefore in this case:

$$F'(v) = [\exp(-ikva) + \exp(ikva)]\, F(v) \tag{6}$$

or

$$F'(v) \sim F(o)\, w_o^2 \exp\left[-2(vw_o)^2\right] \cos^2 kva \tag{7}$$

where "k" is the wavevector, "v" is the angle in the image domain and "a" the distance from the optical axis of the objective to the slits.

The zero minima fringes correspond to:

$$\cos^2 kva = 0 \rightarrow v = \frac{(2p+1)\lambda}{4a} \quad , \; p = 0,1,2,\ldots \tag{8}$$

which yields:

$$a' = s' \sin v = s' \sin\left[\frac{(2p+1)\lambda}{4a}\right] \tag{9}$$

where "s'" is the radius of the image circle through the objective and:

$$m = \frac{s'}{s} = \frac{a'}{a} \tag{10}$$

represents the lateral magnification of the objective.

Using the Lagrange invariant one can write:

$$w_o \sin \theta_{FF} = w_o' \sin \theta'_{FF} \tag{11}$$

where θ_{FF} is the halfangle of divergence in the far-field approximation ($s \gg z_R$) [8]:

$$\theta_{FF} = \arcsin \frac{\lambda}{\pi w_o} \tag{12}$$

and z_R is the Rayleigh range defining the intensity profile along the propagation axis:

$$z_R = \frac{\pi w_o^2}{\lambda} \tag{13}$$

The lateral magnification of the objective can be expressed in terms of image/object waists:

$$m = \frac{w'_o}{w_o} = \{[1 - (\frac{s}{f})]^2 + (\frac{z_R}{f})^2\}^{-1/2} = \frac{s'}{s} \tag{14}$$

where f represents its focal length given by:

$$f = \frac{ss'}{s+s'} \tag{15}$$

From (12) and (14) one can derive the numerical aperture of the objective in the image domain and the theoretical resolution limit (Rayleigh criterion):

$$\rho = \frac{.61\lambda}{NA'} = \frac{.61\lambda}{n\sin\theta'_{FF}} = \frac{.61\pi}{n} w'_o \tag{16}$$

If one takes w_o, s, s' as unknown parameters, for a given magnification then (13), (14) + (15) serve as a system of (2) equations with (3) variables. A third equation can be added taking advantage of the fact that the Fourier transform of a Gaussian function is still a Gaussian function [3]. Under these circumstances the $1/e^2$ truncation rule applied to (5) yields:

$$e^{-2} = w_o^2 \exp\,[-2(v^* w_o)^2] \tag{17}$$

or:

$$v^* = \frac{(1+\ln w_o)^{1/2}}{w_o} \tag{18}$$

where v^* stands for the coordinate angle locating the outer edge of the diffracted wavefront:

$$\tan v^* = \frac{w'_o}{s'} \tag{19}$$

Once w_o, s, s' become completely defined by the above equations, one can specify the radius of the geodesic objective (r_o). The size of it has to accept the angular aperture given by θ_{FF} and therefore:

$$d = 2r_o \geq w(s) = w_o\,[1+(\frac{s}{z_R})^2]^{1/2} \tag{20}$$

4. THE CONTRIBUTION OF THE "NOISE" FACTORS

By "noise" factors we understand herein the perturbative contributions of real parameters on the switch efficiency. We address briefly below only three of them: the spectral width of the beams, the errors related to the spherical aberration and image defocussing.

a) To evaluate the effect of the spectral width of the source one has to start by computing the spread function for wavetrains of finite length [3]:

$$I(v) = \int D(r')\, A^*\,(v\frac{r'}{c})\, \exp\,(ik_o v r')dr' \tag{21}$$

where $A^*(v\frac{r'}{c})$ is the time coherence factor:

$$\begin{cases} A^*(v\frac{r'}{c}) = 1 \text{ for } \Delta\lambda \neq 0 \\ A^*(v\frac{r'}{c}) \neq 1 \text{ for } \Delta\lambda = 0 \end{cases} \tag{22}$$

and D(r') represents the autocorrelation function in amplitudes:

$$D(r') = \int A(r)A(r-r')dr' \tag{23}$$

Because we are dealing with the diffraction through a slit having a Gaussian transmission profile, D(r') is the common part of the two Gaussian plots displaced with r' with respect to one another:

$$\begin{cases} D(r') = A(o)\exp\left[-\frac{(r-r'-w_o)}{w_o}\right]^2 & \text{for } |r| > w_o \\ D(r') = A(o)\exp\left(-\frac{r^2}{w_o^2}\right) & \text{for } r \in [-w_o, w_o] \end{cases} \tag{24}$$

$$\begin{cases} A(r) = A(o)\exp\left(-\frac{r^2}{w_o^2}\right) & \text{for } r \in [-w_o, w_o] \\ A(r) = 1 & \text{for } |r| \in w_o \end{cases}$$

Introducing a new variable $\gamma = \frac{r'}{w_o}$, (21) becomes:

$$I(v) = \int_{-2}^{o} A(o)\exp\left[-(\frac{r}{w_o}-\gamma-1)^2\right](1+\gamma\frac{vw_o}{c\tau})\exp(ik_o v\gamma w_o)\,d\gamma + \tag{25}$$
$$+ \int_{o}^{2} A(o)\exp\left(-\frac{r^2}{w_o^2}\right)(1-\gamma\frac{vw_o}{c\tau})\exp(ik_o v\gamma w_o)d\gamma$$

where:

$$\tau = (\Delta\nu)^{-1} \quad , \quad \nu_o = c\lambda_o^{-1} \quad \text{and} \quad k_o = 2\pi\lambda_o^{-1} \tag{26}$$

By processing (25) one may show that I (v) contains the basic spread function for a perfect monochromatic wavefront (5) plus a perturbative contribution due to the spectral width.

b) When spherical aberration is not well balanced, the spot energy is being redistributed amoung the diffraction rings. This makes the contrast softer and generates losses of radiant energy through the switch. If a certain amount of marginal spherical aberration is present (LA_m), then the blur spot size can be evaluated with [10]:

$$\rho \sim .50\, LA_m \tan U_m \tag{27}$$

where U_m is the ray slope in the image domain, or with:

$$\rho \sim .84\ LA_z \tan U_m \tag{28}$$

when the marginal spherical is corrected to zero (LA_m=0).

c) The depth of focus associated with the use of the planar optics can be derived starting from (20). Allowing a prescribed expansion of the beam radius with respect to the waist:

$$q = \frac{w(s)}{w_o} \tag{29}$$

and solving for the depth Δs, one gets:

$$\Delta s = \pm \frac{\pi w_o^2}{\lambda} (q^2-1)^{1/2} \tag{30}$$

This formula sets the upper limit of the defocussing error.

5. DESCRIPTION OF THE HIGH RESOLUTION TARGET

As shown in Fig. 5 the high resolution target represents a core-cladded spherical lens. Basically a gradient index core is cladded with an additional layer having a constant refractive index.

This lens has the property of imaging a point source onto a diffraction limited spot size [6]. The refractive index is described by the function:

$$\begin{aligned} n^2(r) &= n^2(o)\ [1 + G_2(\frac{r}{r_o})^2 + G_4(\frac{r}{r_o})^4] && \text{for } r_o \geq r > o \\ n(r) &= \text{constant} && \text{for } R \geq r > r_o \end{aligned} \tag{31}$$

where G_2 and G_4 are the so-called profile coefficients.

Under standard operating conditions a collimated incident beam is focussed outside the clad. By extension, in our approach the core cladded target images an intermediate object "F_1" onto a spot located on the edge of the clad (F_2"). As mentioned earlier, this becomes the object for the pick-up relay "R_3".

The target can be designed in several alternate ways (combination of mode index lenses or a generalized Luneburg lens) provided that it achieves diffraction limited performance and a minimum loss of radiant energy.

6. AN ALTERNATE CONSTRUCTION OF THE SWITCH

Because aspheric geodesic lenses are difficult to fabricate, an alternate construction of the planar optics is desirable.

The configuration presented in Fig. 6 uses overlay corrected lenses consisting of a spherical depression surrounded by an area of higher refractive index. This setup can approach diffraction limited performance for on-axis beams at $\theta \leq 2^o$ when the design allows correction of the spherical aberration over 90% of the lens diameter [9].

7. INTEGRATION OF THE SWITCH IN A LOGIC PROCESSOR

Using the formula of the beam intensity along the optical axis

$$I(0) = \frac{2P}{\pi w^2(s)} \tag{32}$$

one can see that the total drop of the intensity through the switch is the sum between the physical attenuation of the beam (absorption, scattering, vignetting, reflection) and the change due to divergence at the target location. Let "ε" designate the transmission efficiency per switch. If one considers a discrete sequence of "N" switches and assumes that "ε" enters as a constant parameter per switch, then the intensity on axis drops following the iteration:

$$\begin{aligned} I_1 &= \frac{2P}{\pi w_o^2} \\ I_2 &= \varepsilon w_o'^2 I_1 = \varepsilon m^2 w_o^2 I_1 \\ I_3 &= \varepsilon^2 m^6 w_o^4 I_1 \\ &\cdot \\ &\cdot \\ I_N &= \varepsilon^{N-1} m^{N(N-1)} w_o^{2(N-1)} I_1 \end{aligned} \tag{33}$$

The incremental variation in intensity becomes:

$$\Delta I_N = I_{N+1} - I_N = I_1 \underbrace{(1 - \varepsilon^{-1} w_o^{-2})\ (\varepsilon w_o^2)^N m^{N^2}}_{\Phi(\varepsilon, w_o, m, N)} \Delta N \tag{34}$$

$(\Delta N = 1)$

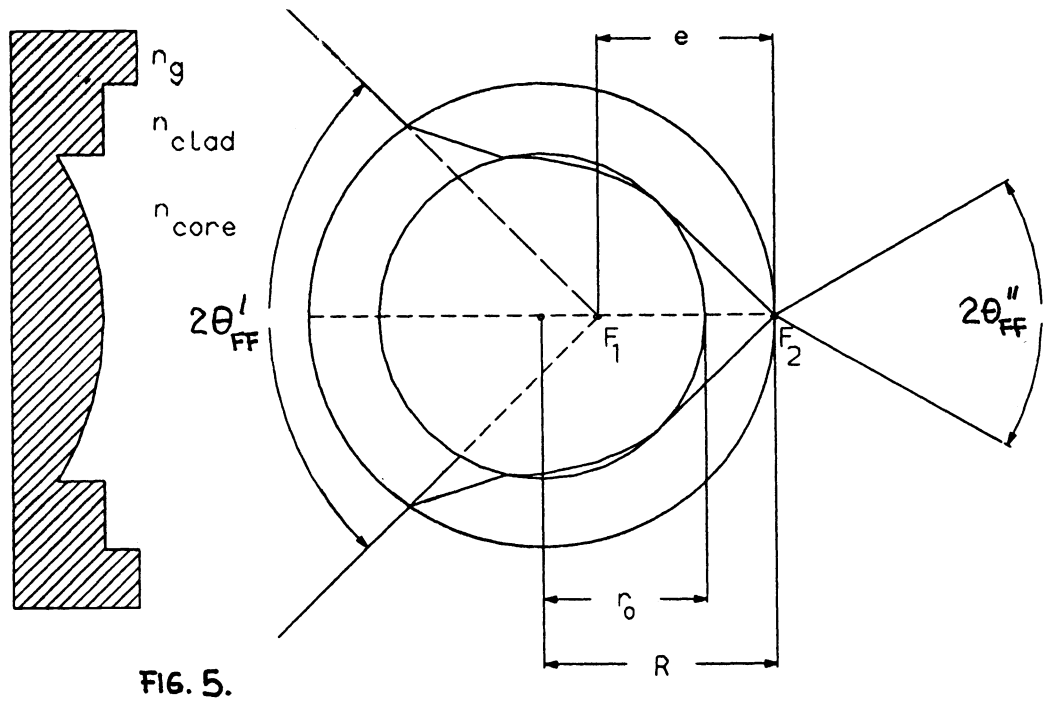

FIG. 5.

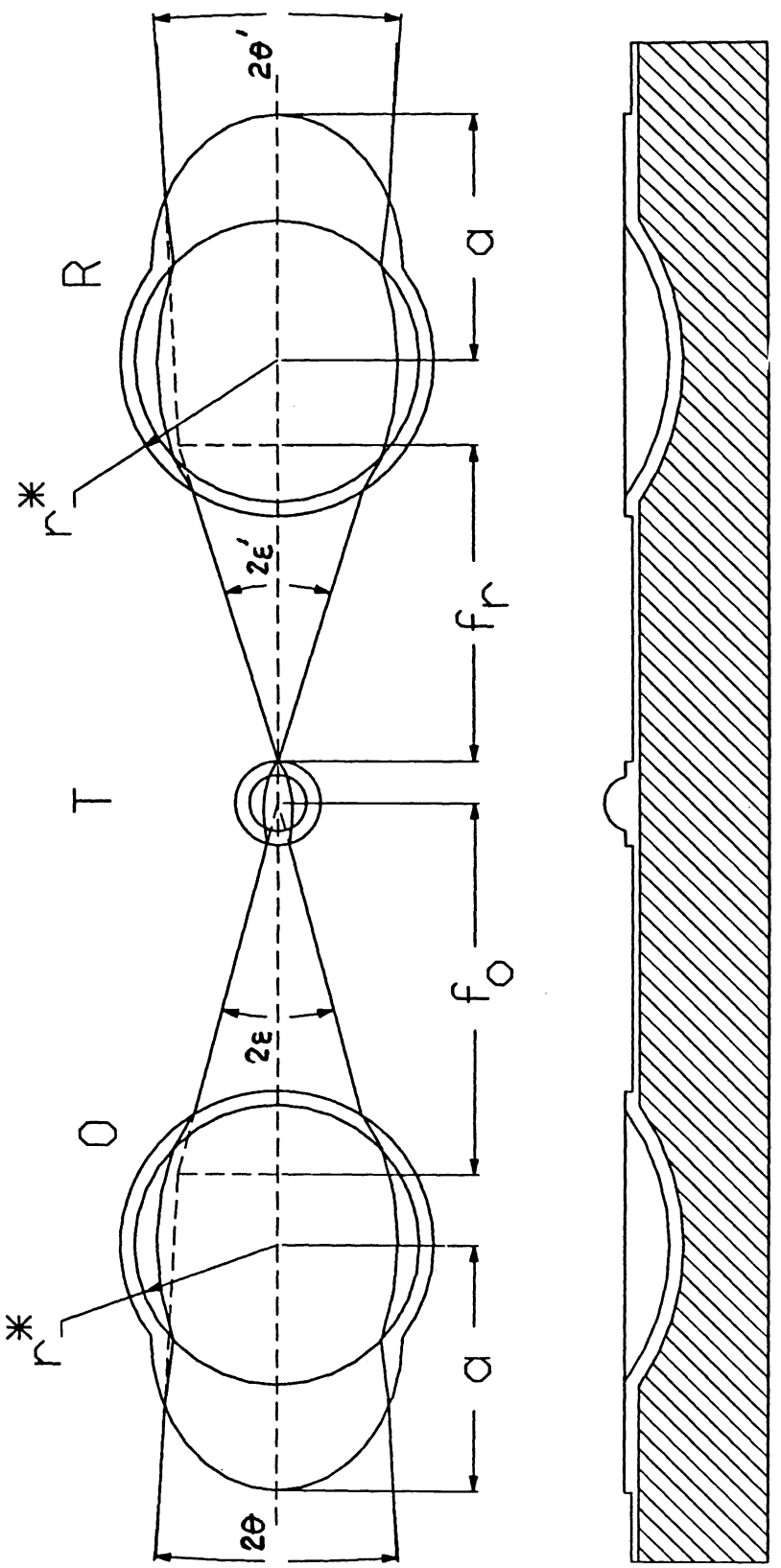

FIG.6

Passing to a differential form (N>>1) (34) yields:

$$\frac{\Delta I}{I_1} = \int_1^N \Phi(\varepsilon, w_o, m, N)dN \qquad (35)$$

which defines the analytical damping curve of the beam intensity on axis.

In order to avoid any confusion in decoding the logical value of a damped signal, the beam intensity must be regenerated (Fig. 7). The simplest way to achieve this amplification is to place a photonic switch close to the location where the signal approaches I_{1m}. It is apparent that the gap between I_{0M} and I_{1m} provides the internal consistency of the computing process, since all signals with $I \leq I_{0M}$ have a "0" logical value.

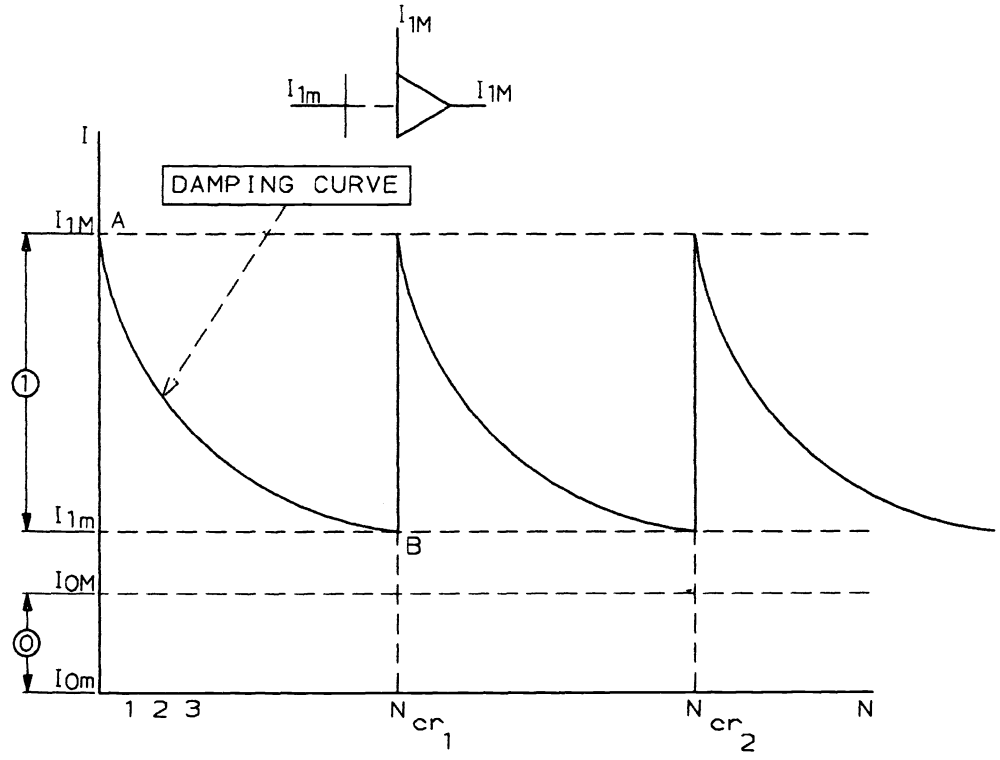

FIG.7

8. REFERENCES

1. N. Peyghambarian, H.M. Gibbs, "Optical bistability for optical signal processing and computing", OE, vol. 24/1, p. 68.

2. Y. Imai, Y. Ohtsuka, "Optical computing based on interference fringe shifting", OE, vol. 25/1, p. 98.

3. M. Francon, Diffraction - Coherence in Optics, Pergamon Press, 1966, p. 46.

4. "Optics Guide 4", Melles Griot, 17-15.

5. N. Saga et al., "Diffraction of a Gaussian beam through a finite aperture lens and the resulting heterodyne efficiency", AO, vol. 20/16, p. 2827.

6. K. Kikuchi et al., "Cladded radially inhomogeneous sphere lens", AO, vol. 20/3, p. 388.
7. S. Sottini et al., "General solution of the problem of a perfect geodesic lens for integrated optics", JOSA, 69/9, p. 1248.
8. S. Self, "Focussing of spherical Gaussian beams", AO, vol. 22/5, p. 658.
9. G. Betts, G.E. Marx, "Spherical aberration correction and fabrication tolerances in geodesic lenses", AO, vol. 17/24, p. 3969.
10. W. Smith, Modern Optical Engineering, McGraw-Hill, 1966, p. 305.
11. S. Doric, E. Munro, "General solution of the nonfull aperture Luneburg lens problem", JOSA, vol. 73/8, 1983, p. 1083.
12. G.W. Stroke, An Introduction to Coherent Optics and Holography, Academic Press, 1966, p. 64.
13. Lipson & Lipson, Optical Physics, Cambridge Univ. Press, 1969, p.160.